



## Short communication

## Co-sinterable lithium garnet-type oxide electrolyte with cathode for all-solid-state lithium ion battery



Shingo Ohta\*, Juntaro Seki, Yusuke Yagi, Yuki Kihira, Takao Tani, Takahiko Asaoka

Toyota Central R&amp;D Labs. Inc., 41-1 Yokomichi, Nagakute, Aichi 480-1192, Japan

## HIGHLIGHTS

- The sintering temperature of garnet electrolyte was found to significantly lower by addition.
- The simultaneous interdiffusion of elements was important to lower sintering temperature.
- Garnet oxide exhibited high lithium ion conductivity despite of the low sintering temperature.
- All-solid-state lithium ion battery using garnet oxide was fabricated by co-sintering.

## ARTICLE INFO

## Article history:

Received 3 February 2014

Received in revised form

11 April 2014

Accepted 14 April 2014

Available online 24 April 2014

## Keywords:

Solid electrolyte

Garnet oxide

All-solid-state lithium ion battery

Co-sintering

Lithium ion conductor

## ABSTRACT

We investigated the development of a novel lithium garnet-type oxide electrolyte, which is co-sinterable with a metal oxide cathode, for practical all-solid-state lithium ion batteries using metal oxide electrolytes. The sintering temperature of  $\text{Li}_{6.8}(\text{La}_{2.95}\text{Ca}_{0.05})(\text{Zr}_{1.75}\text{Nb}_{0.25})\text{O}_{12}$  was found to significantly lower to 790 °C by addition of  $\text{Li}_3\text{BO}_3$  and  $\text{Al}_2\text{O}_3$ , due to simultaneous interdiffusion of Al and Ca elements between garnet-type oxide and additives. The sintered electrolyte exhibited high lithium ion conductivity of  $0.36 \text{ mS cm}^{-1}$  at 25 °C despite of the low sintering temperature. An all-solid-state lithium ion battery was successfully prepared by co-sintering of the electrolyte and  $\text{LiCoO}_2$  (cathode), followed by coating of Li metal (anode), and confirmed to function well as a secondary battery with charge and discharge capacities of 98 and 78 mAh  $\text{g}^{-1}$ , respectively. These results opened the potential for fabrication of all-solid-state lithium ion batteries by a simple and well-established co-sintering process.

© 2014 Elsevier B.V. All rights reserved.

## 1. Introduction

Lithium ion secondary batteries have been widely used as power sources for electric vehicle (EV), a mobile phone and etc., and are now indispensable for our daily lives. At the same time, safety of the batteries has been becoming an important issue with the progress of their performance (e.g. capacity and energy density). From this viewpoint, all-solid-state lithium ion batteries using solid electrolytes have attracted much attention as a next-generation battery due to non-use of flammable organic liquid electrolytes.

Especially, specific focus has been placed on “metal oxide” electrolytes rather than others (e.g. sulfide electrolyte) because metal oxides are stable in air and thus never release toxic gases even in case of breaking down. In addition, metal oxide electrolyte has several advantages such as high chemical and thermal stability and

a low charge transfer resistance between the electrode/electrolyte interfaces [1–3]. Furthermore, metal oxide electrolyte/electrode systems have a great merit to construct a bi-polar structure for high capacity, because a layer-by-layer structure of electrolyte, electrode and metal is easily fabricated by a simple co-sintering process, which has been widely used in production of multi-layered ceramic capacitors. However, low lithium ion conductivities of metal oxide electrolytes (e.g.  $1 \mu\text{S cm}^{-1}$  at R.T.) limited their use for all-solid-state batteries.

The important breakthrough in this field was achieved in 2007 by R. Murugan, who first reported  $\text{Li}_7\text{La}_3\text{Zr}_2\text{O}_{12}$  (LLZO) and its derivatives with high lithium ion conductivity ( $\sim 0.1 \text{ mS cm}^{-1}$  at R.T.) [4–13]. The discovery motivated researches on the use of metal oxide electrolytes for all-solid-state batteries. We also investigated the electrochemical performance of a model battery using an as-sintered Nb doped LLZO (LLZO-Nb,  $0.8 \text{ mS cm}^{-1}$  at 25 °C) pellet and  $\text{LiCoO}_2$  (LCO, one of typical cathodes), and found that the model battery exhibited good charge–discharge capacities and low interfacial resistance between LCO and LLZO-Nb comparable with

\* Corresponding author. Tel.: +81 561 71 7659; fax: +81 561 71 5743.

E-mail address: [sohta@mosktytlabs.co.jp](mailto:sohta@mosktytlabs.co.jp) (S. Ohta).

that of lithium ion batteries with liquid organic electrolytes [2,14]. The results confirmed the availability of LLZO-Nb as a metal oxide electrolyte for all-solid-state batteries. The next challenge is co-sintering of electrolyte and electrode materials with high densities but without the formation of other compounds by interdiffusion.

Here, we investigated the design of LLZO-Nb for co-sintering with LCO (cathode) for the first step because it is one of the most important issues to suppress the reaction of LLZO-Nb and cathode by drastically lowering the sintering temperature of LLZO-Nb to less than 900 °C [15]. In order to overcome this difficulty, our strategy is to enhance interdiffusion between LLZO-Nb and a grain boundary phase (not LCO) by an appropriate selection of additives. As the result, addition of  $\text{Al}_2\text{O}_3$  and  $\text{Li}_3\text{BO}_3$  to Ca and Nb doped LLZO (LLZO-CaNb) lowered the sintering temperature to 790 °C with maintaining high lithium ion conductivity but without the reaction with LCO. The developed electrolyte pellet was stacked on a LCO (cathode) pellet, co-sintered at 790 °C and coated with Li metal (anode). The obtained model battery was confirmed to work properly with charge–discharge capacities of 72% and 58%, respectively, to the theoretical value. The present results opened the potential to produce all-solid-state lithium ion battery by a simple co-sintering process.

## 2. Experimental

Commercial reagents were purchased from Sigma–Aldrich and Kojundo Chemical Lab. Co. Ltd. and used as received for  $\text{Li}(\text{OH})$ ,  $\text{La}(\text{OH})_3$ ,  $\text{Ca}(\text{OH})_2$ ,  $\text{ZrO}_2$ ,  $\text{Nb}_2\text{O}_5$ ,  $\text{Li}_2\text{CO}_3$ ,  $\text{B}_2\text{O}_3$  and  $\gamma\text{-Al}_2\text{O}_3$ . LLZO-CaNb was prepared by conventional solid state reactions. The starting materials,  $\text{Li}(\text{OH})$ ,  $\text{La}(\text{OH})_3$ ,  $\text{Ca}(\text{OH})_2$ ,  $\text{ZrO}_2$ , and  $\text{Nb}_2\text{O}_5$  were mixed by planetary ball-milling, and then calcined at 700 °C for 48 h. The composition of the samples were evaluated by inductively coupled plasma spectroscopy (ICP; Rigaku Co. CIRIOS 120 EOP).  $\text{Li}_3\text{BO}_3$  powder as an additive was prepared by heating a mixture of  $\text{Li}_2\text{CO}_3$  and  $\text{B}_2\text{O}_3$  at 600 °C. The calcined LLZO-CaNb powder was mixed with the additives (both  $\text{Al}_2\text{O}_3$  and  $\text{Li}_3\text{BO}_3$ , only  $\text{Al}_2\text{O}_3$  or only  $\text{Li}_3\text{BO}_3$ ) by planetary ball-milling. The mixture was die-pressed at 10 MPa into a pellet (green density: ca. 40% ( $2.10 \text{ g cm}^{-3}$ )) and sintered at 790 °C for 40 h in air. The crystal structure and the lattice parameter of the samples were evaluated by X-ray diffraction (XRD; Rigaku Co. Ultima IV,  $\text{CuK}\alpha$  radiation, 40 kV, 30 mA). The electrical conductivity of the samples was measured using a two-probe AC impedance method (Agilent 4294A) in the frequency range of 110 MHz–40 Hz from 25 to 150 °C. The distribution of the elements was measured by EPMA (JEOL Ltd. JXA-8500F). The cathode/electrolyte stacked pellet was prepared by co-sintering process. A commercial  $\text{LiCoO}_2$  powder (average particle size: 5  $\mu\text{m}$ , Nippon Chemical Industrial Co., Ltd.) as a cathode was mixed with  $\text{Li}_3\text{BO}_3$  and the calcined LLZO-CaNb powder in the ratio of 42:35:23 (wt%). The mixed powder was put on the LLZO-CaNb electrolyte pellet and co-die-pressed at 10 MPa. The stacked pellet was sintered at 790 °C in air. The morphology and the elemental distribution of the cathode/electrolyte interface were observed by FIB-SEM (Hitachi NB5000 FIB-SEM, 5 kV) and EDX (EDAX Inc. GenesisAPEX2), respectively. The charge–discharge curves were obtained using a potentiostat galvanostat (Solartron 1480) under galvanostatic conditions of  $1 \mu\text{A g}^{-1}$  (rate:  $\sim 0.01\text{C}$ ) in the range from 3.0 to 4.2 V.

## 3. Results and discussions

$\text{Li}_{6.8}(\text{La}_{2.95}\text{Ca}_{0.05})(\text{Zr}_{1.75}\text{Nb}_{0.25})\text{O}_{12}$  (LLZO-CaNb) was chosen as the base garnet-type oxide compound due to its high lithium ion conductivity ( $\sim 0.6 \text{ mS cm}^{-1}$  at 25 °C) and lower sintering

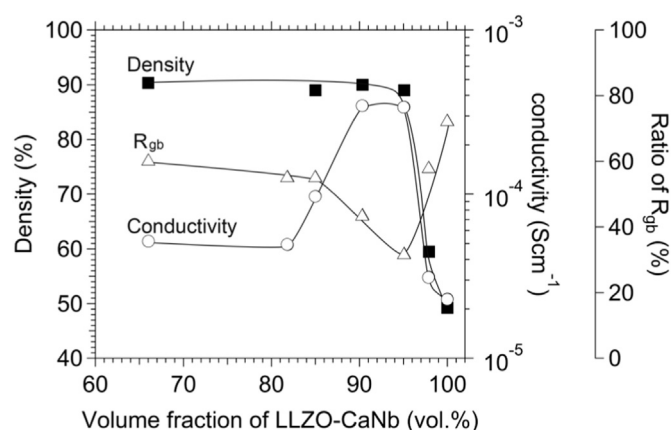


Fig. 1. Effects of  $\text{Li}_3\text{BO}_3$  addition on density (square), lithium ion conductivity (open circle) and the ratio of resistance due to grain boundary (open triangle) for LLZO-CaNb with  $\text{Al}_2\text{O}_3$  (0.2 mol%).

temperature (1050 °C) than those of other lithium garnet-type oxides [16]. The composition ratio of  $\text{Li/La/Ca/Zr/Nb}$  in calcined LLZO-CaNb powder which was evaluated by ICP was 6.81/2.96/0.05/1.75/0.25, where this ratio was normalized according to Zr at 1.75.  $\text{Al}_2\text{O}_3$  and  $\text{Li}_3\text{BO}_3$  were selected as additives for lowering the sintering temperature due to the following reasons. The  $\text{Al}^{3+}$  ion can be substituted to the  $\text{Li}^+$  site in LLZO-CaNb by interdiffusion into the LLZO-CaNb grain, which can improve the sinterability of LLZO-CaNb. The  $\text{Al}^{3+}$  ion was added until its solubility limit (0.2 mol %) to LLZO-CaNb [17–19].  $\text{Li}_3\text{BO}_3$  can form a liquid phase due to its low melting point (ca. 700 °C) and thus enhance liquid phase sintering of LLZO-CaNb without reactions with it [20]. The effects of  $\text{Li}_3\text{BO}_3$  addition on sinterability and lithium ion conductivity were preliminarily evaluated for LLZO-CaNb with  $\text{Al}_2\text{O}_3$  (0.2 mol%) is shown in Fig. 1. The addition of  $\geq 5$  vol.% was effective for densification, whereas the addition of  $> 10$  vol.% resulted in the decrease of the lithium ion conductivity due to the large increase of the grain boundary resistance. This can be explained by the mechanism that  $\text{Li}_3\text{BO}_3$  tends to exist at the grain boundaries in addition to the triple points, which leads to insufficient contact between LLZO-CaNb grains. Thus, the amount of  $\text{Li}_3\text{BO}_3$  addition was determined as 5–10 vol.% to LLZO-CaNb according to these results.

Sinterability of LLZO-CaNb was drastically improved by co-addition of  $\text{Al}_2\text{O}_3$  and  $\text{Li}_3\text{BO}_3$ . Table 1 lists the relative densities for die-pressed pellets of a calcined LLZO-CaNb powder with or without the additives (both  $\text{Al}_2\text{O}_3$  and  $\text{Li}_3\text{BO}_3$ , only  $\text{Al}_2\text{O}_3$ , only  $\text{Li}_3\text{BO}_3$  and no additives) after sintering at 790 °C in air. It is clear that (i) the formation of a liquid phase (addition of  $\text{Li}_3\text{BO}_3$ ) is effective for densification of LLZO-CaNb and (ii) the relative density increases up to nearly 90% only in the case of co-addition of  $\text{Al}_2\text{O}_3$  and  $\text{Li}_3\text{BO}_3$ . The XRD pattern of all the diffraction peaks confirmed the formation of a cubic garnet type structure (space group:  $Ia\text{-}3d$ , JCPDS: 84-1753) with the lattice parameter of 12.95 Å (Fig. 2). The ICP analysis showed that the composition ratio of  $\text{Li/La/Ca/Zr/Nb/}$

Table 1  
Relative density and lithium ion conductivity of the samples.

Base	Additive	Rel. dens. (%) <sup>a</sup>	$\text{Li}^+ \sigma$ ( $\text{mS cm}^{-1}$ )
LLZO-CaNb	$\text{Al}_2\text{O}_3$ , $\text{Li}_3\text{BO}_3$	90	0.36
LLZO-CaNb	—	49	0.004
LLZO-CaNb	$\text{Al}_2\text{O}_3$	49	0.008
LLZO-CaNb	$\text{Li}_3\text{BO}_3$	52	0.006

<sup>a</sup> The theoretical density was calculated based on the ideal densities of LLZO-CaNb ( $5.08 \text{ g cm}^{-3}$ ) and LBO ( $2.16 \text{ g cm}^{-3}$ ) and their mixing ratio (90/10) in volume.

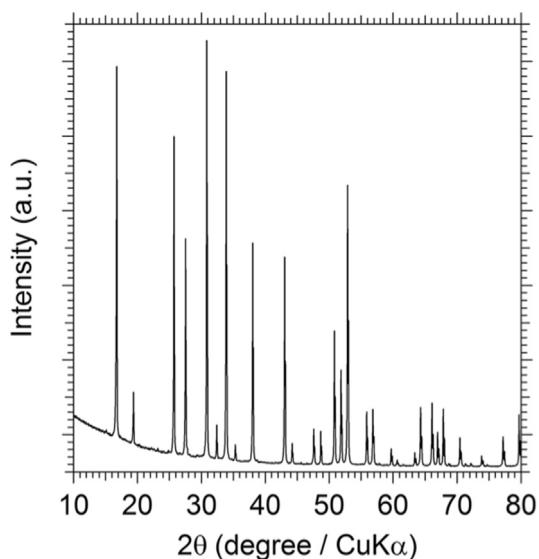


Fig. 2. XRD pattern of LLZO-CaNb with co-addition of  $\text{Al}_2\text{O}_3$  and  $\text{Li}_3\text{BO}_3$  sintered at 790 °C.

Al/B in sintered LLZO-CaNb with co-addition of  $\text{Al}_2\text{O}_3$  and  $\text{Li}_3\text{BO}_3$  was 7.55/2.95/0.31/1.75/0.25/0.19/0.22, normalized according to Zr at 1.75.

Electron probe microanalysis (EPMA) was conducted in order to unravel the mechanism of the improvement of the sinterability by co-addition of  $\text{Al}_2\text{O}_3$  and  $\text{Li}_3\text{BO}_3$  (Fig. 3). It is of interest that (i) the Al element is homogeneously distributed in the LLZO-based grains whereas (ii) the Ca and B elements are located in the triple points [21]. The results indicate that the Al element, initially located out of the LLZO-CaNb crystals, diffuses into the LLZO-based grains while the Ca element, initially located in the LLZO-CaNb crystals, diffuses into the  $\text{Li}_3\text{BO}_3$ -based triple points during sintering, as shown as the following chemical equation.



Table 2

Relative density and lithium ion conductivity of the samples.

Base	Additive	Rel. dens. (%) <sup>a</sup>	$\text{Li}^+ \sigma$ ( $\text{mS cm}^{-1}$ )
LLZO-AlNb	$\text{CaO}$ , $\text{Li}_3\text{BO}_3$	76	0.09
LLZO-Nb	$\text{Al}_2\text{O}_3$ , $\text{Li}_3\text{BO}_3$	72	0.08

<sup>a</sup> The theoretical density was calculated based on the ideal densities of LLZO-CaNb ( $5.08 \text{ g cm}^{-3}$ ) and LBO ( $2.16 \text{ g cm}^{-3}$ ) and their mixing ratio (90/10) in volume.

The simultaneous interdiffusion between the garnet-type oxide and the additives in addition to the formation of a liquid phase is considered to significantly improve the sinterability of LLZO-CaNb. The importance of the simultaneous interdiffusion during sintering was further confirmed by two additional experiments. Table 2 lists the relative densities and lithium ion conductivity of the sintered sample for the LLZO-Nb (based garnet-type oxide)/(CaO and  $\text{Li}_3\text{BO}_3$ ) (additives) and LLZO-Nb based garnet-type oxide)/(CaO and  $\text{Li}_3\text{BO}_3$ ) (additives) after sintering at 790 °C. The relative density of the sintered sample was 76% for the LLZO-AlNb (base garnet-type oxide)/(CaO and  $\text{Li}_3\text{BO}_3$ ) (additives) system, which suggests that the simultaneous interdiffusion rather than the final compositions of the grain and the triple points is crucial for the densification. In addition, the density of the sintered sample was 72% for the LLZO-Nb (base garnet-type oxide)/(Al $_2$ O $_3$  and  $\text{Li}_3\text{BO}_3$ ) (additives) system, which suggests that the diffusion of both the Al and Ca elements are necessary for the densification.

The developed LLZO-AlNb in this study was confirmed to exhibit high lithium ion conductivity ( $0.36 \text{ mS cm}^{-1}$  at R.T.), comparable to those of LLZO-based materials sintered at high temperature (1000–1200 °C), despite of the low sintering temperature of 790 °C. Fig. 4a shows the Nyquist plots at 25 °C for the developed LLZO-AlNb and LLZO-AlNb prepared by a conventional process (sintered at 1150 °C, abbreviated as LLZO-AlNb-conv.). Two semicircles at higher and lower frequencies, which were observed in both samples, are assigned to the bulk resistance ( $R_b$ ) and the grain boundary resistance ( $R_{gb}$ ), respectively [9]. The  $R_b$  was 2.1 and 2.0 kΩ cm and the  $R_{gb}$  was 0.53 and 0.48 kΩ cm for the developed LLZO-AlNb and LLZO-AlNb-conv., respectively. The calculated lithium ion conductivity of the developed LLZO-AlNb ( $0.36 \text{ mS cm}^{-1}$ ) was almost same

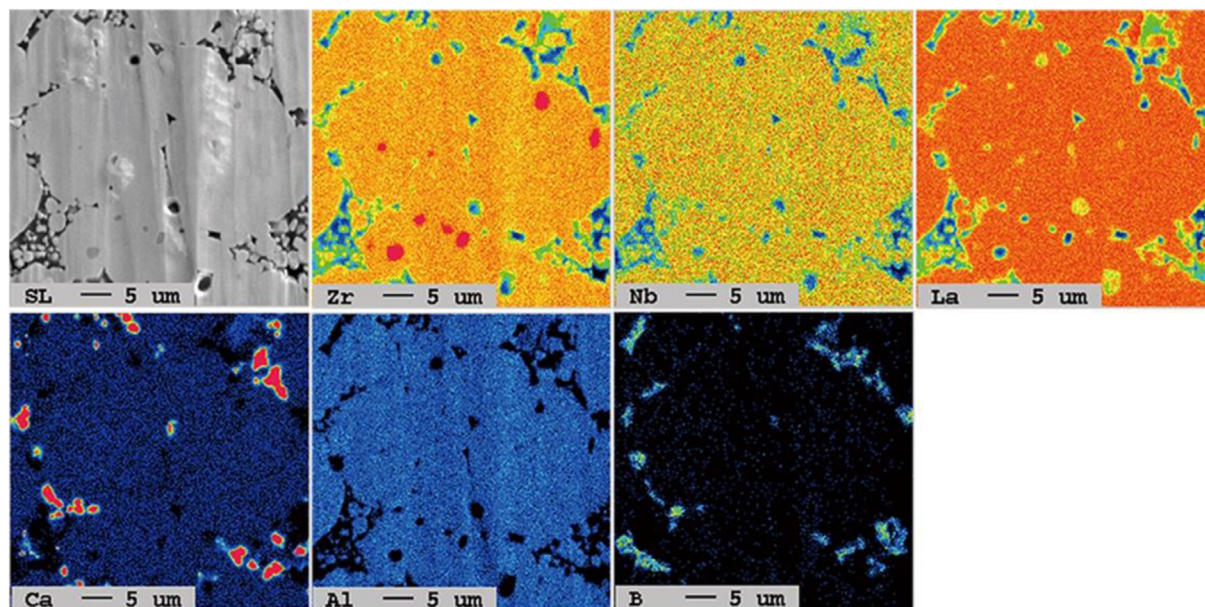
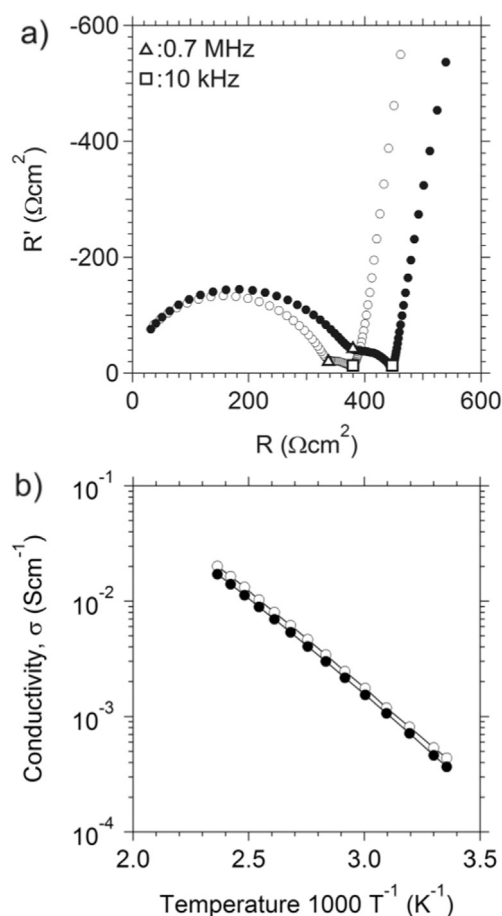
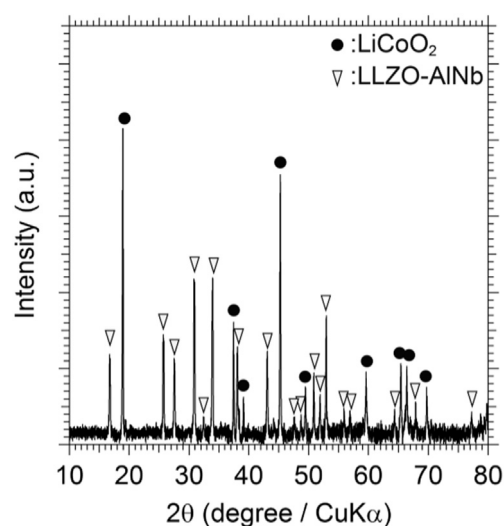


Fig. 3. Cross-sectional EPMA mapping images of LLZO-CaNb with co-addition of  $\text{Al}_2\text{O}_3$  and  $\text{Li}_3\text{BO}_3$  sintered at 790 °C.





**Fig. 4.** a) Nyquist plots (110 MHz–40 Hz) of the developed LLZO-AlNb (solid circle) and LLZO-AlNb prepared by a conventional process (sintered at 1150 °C) (open circle). b) Temperature dependences (25–150 °C) of lithium ion conductivity of these samples.



**Fig. 6.** XRD pattern of co-sintered LLZO-AlNb and LCO.

as that of LLZO-AlNb-conv. ( $0.4 \text{ mS cm}^{-1}$ ). In addition, the termination points of the semicircles were 0.7 MHz and 1.0 kHz for  $R_b$  and  $R_{gb}$ , respectively, for the both samples. These results suggest that the conduction path of Li ions between grains is sufficiently formed for the developed LLZO-AlNb despite of the low sintering temperature (790 °C). Fig. 4b shows temperature dependences of lithium ion conductivity for the developed LLZO-AlNb and LLZO-AlNb-conv. The lithium ion conductivities were linear and obeyed the Arrhenius law ( $\sigma = A\exp(-E_a/kT)$ , where  $A$  is the frequency factor,  $k$  is the Boltzmann constant,  $T$  is the absolute temperature, and  $E_a$  is the activation energy). The  $E_a$  for the developed LLZO-AlNb was  $\sim 31 \text{ kJ mol}^{-1}$ , which is almost the same as that of LLZO-AlNb-conv. and also the reported values [12].

Chemical stability of LLZO-AlNb with LCO during co-sintering was confirmed by focused ion beam scanning electron

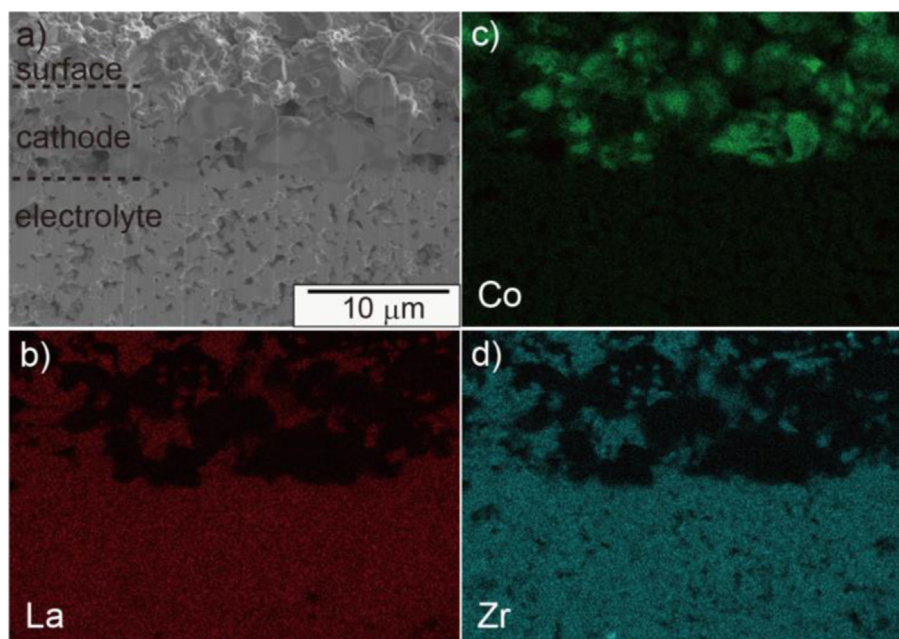


**Fig. 5.** a) Cross-sectional SEM (secondary electron) image of the cathode/electrolyte interface and EDX mapping images of b) La, c) Co and d) Zr.

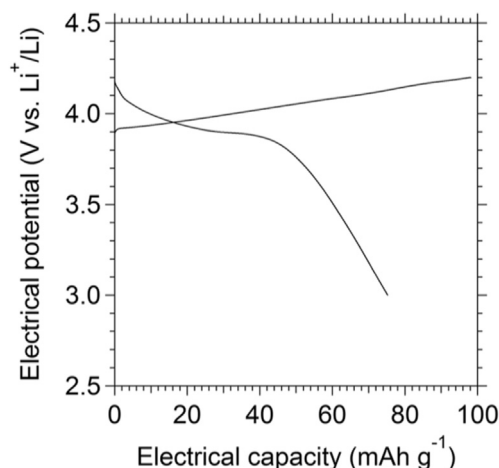


Fig. 7. Charge–discharge curves for the co-sintered model battery. The horizontal axis shows the capacity normalized by the weight of the  $\text{LiCoO}_2$  cathode.

microscope (FIB-SEM), energy dispersive X-ray analysis (EDX) and XRD. The sample was prepared by stacking of the mixed LCO and LLZO-AINb cathode layer (thickness:  $\sim 10 \mu\text{m}^t$ ) onto the developed LLZO-AINb electrolyte layer (thickness:  $\sim 1.0 \text{ mm}^t$ ), followed by co-sintering at  $790^\circ\text{C}$ . The cross-sectional SEM image and EDX mapping of the cathode/electrolyte interface is shown in Fig. 5. The interface of LCO grains and LLZO-AINb grains was primarily well-sintered although a few voids existed. The voids can be formed by capillary action of  $\text{Li}_3\text{BO}_3$  in the liquid phase to the more porous LLZO-AINb electrolyte during co-sintering. The EDX mapping confirmed that no elemental diffusion occurred between LCO and LLZO-AINb. The XRD pattern of the cathode layer showed only diffraction peaks of LCO (JCPDS: 50-0653) and LLZO-AINb (Fig. 6). These results indicate that no chemical reaction between LCO and LLZO-AINb occurred at the co-sintering process.

Finally, the developed LLZO-AINb was confirmed to work well as an electrolyte of an all-solid-state lithium ion battery. The model battery was constructed by coating of Li metal on the electrolyte side of the co-sintered cathode (LLZO-AINb + LCO)/electrolyte (LLZO-AINb) pellet, and its battery performance was evaluated. Fig. 7 shows charge–discharge curves of the model battery. The charge curve started at 3.9 V and the plateau of the discharge curve was observed at approximately 3.9 V. These behaviors are typical for the extraction/insertion reaction of LCO and thus the cathode/electrolyte pellet is considered to work properly. However, the charge and discharge capacities of this battery were 98 and  $78 \text{ mA h g}^{-1}$ , respectively, which correspond to about 72 and 58% of the theoretical capacity [22,23]. In addition, the electrical potential at the end of discharge gradually dropped due to the polarization in cathode layer. These results suggest that the formation of the lithium ion conduction path is not enough in the cathode/electrolyte pellet and thus optimization of the processing (e.g. powder preparation and co-sintering conditions) is necessary to improve the battery performance.

#### 4. Conclusions

We developed a novel lithium garnet-type oxide electrolyte which is densified to 90% in relative density at  $790^\circ\text{C}$  and exhibits a high lithium ion conductivity of  $0.36 \text{ mS cm}^{-1}$  at  $25^\circ\text{C}$ . Addition of  $\text{Li}_3\text{BO}_3$  and  $\text{Al}_2\text{O}_3$  to LLZO-CaNb was found to effectively enhance the sintering by simultaneous interdiffusion of Al and Ca elements between garnet-type oxide and additives. The developed electrolyte was successfully co-sintered with LCO without any reactions between them. The model battery using the developed electrolyte was confirmed to function well as a secondary battery with charge and discharge capacities of 98 and  $78 \text{ mA h g}^{-1}$ , respectively. These results opened the potential for fabrication of all-solid-state lithium ion batteries using metal oxide electrolytes by a simple and well-established co-sintering process.

#### Acknowledgments

This work was financially supported by Applied and Practical LiB Development for Automobile and Multiple Application from the New Energy and Industrial Technology Department Organization (NEDO) in Japan.

#### References

- [1] Y. Iriyama, T. Kako, C. Yada, T. Abe, Z. Ogumi, J. Power Sources 146 (2005) 745.
- [2] S. Ohta, T. Kobayashi, J. Seki, T. Asaoka, J. Power Sources 202 (2012) 332.
- [3] N. Kuwata, N. Iwaguma, Y. Tanji, Y. Matsuda, J. Kawamura, J. Electrochem. Soc. 157 (2010) A521.
- [4] R. Murugan, V. Thangadurai, W. Weppner, Angew. Chem. Int. Ed. 46 (2007) 7778.
- [5] V. Thangadurai, W. Weppner, Adv. Funct. Mater. 15 (2005) 107.
- [6] V. Thangadurai, W. Weppner, J. Power Sources 142 (2005) 339.
- [7] R. Murugan, V. Thangadurai, W. Weppner, Ionics 13 (2007) 195.
- [8] J. Awaka, N. Kijima, H. Hayakawa, J. Akimoto, J. Solid State Chem. 182 (2009) 2046.
- [9] S. Ohta, T. Kobayashi, T. Asaoka, J. Power Sources 196 (2011) 3342.
- [10] H. Xie, K.S. Park, J. Song, J.B. Goodenough, Electrochem. Commun. 19 (2012) 135.
- [11] A. Logéata, T. Köhler, U. Eisele, B. Stiasny, A. Harzera, M. Tovar, A. Senyshyn, H. Ehrenberg, B. Kozinsky, Solid State Ionics 206 (2012) 33.
- [12] J.L. Allena, J. Wolfenstine, E. Rangasamy, J. Sakamoto, J. Power Sources 206 (2012) 315.
- [13] G.T. Hitz, E.D. Wachsman, V. Thangadurai, J. Electrochem. Soc. 160 (2013) A1248.
- [14] S. Ohta, S. Komagata, J. Seki, T. Saeki, S. Morishita, T. Asaoka, J. Power Sources 238 (2013) 53.
- [15] In our preliminary assessment, the sintering temperature of LLZO-Nb is  $1150^\circ\text{C}$ , which is far higher than the chemical reaction temperature ( $\sim 900^\circ\text{C}$ ) of LLZO-Nb with LCO, resulting in the formation of other compounds.
- [16] Y. Kihira, S. Ohta, H. Imagawa, T. Asaoka, ECS Electrochem. Lett. 2 (2013) A56.
- [17] A. Düvel, A. Kuhn, L. Robben, M. Wilkening, P. Heitjans, J. Phys. Chem. C 116 (2012) 15192.
- [18] E. Rangasamy, J. Wolfenstine, J. Allen, J. Sakamoto, J. Power Sources 230 (2013) 261.
- [19] A.A. Hubaud, D.J. Schroeder, B. Key, B.J. Ingram, F. Dogana, J.T. Vaughey, J. Mater. Chem. A 1 (2013) 8813.
- [20] K. Tadanaga, R. Takano, T. Ichinose, S. Mori, A. Hayashi, M. Tatsumisago, Electrochem. Commun. 33 (2013) 51.
- [21] The chemical composition of sintered garnet-type oxide was estimated from EPMA and ICP results is  $(\text{Li}_{6.18}\text{Al}_{0.19})(\text{La}_3)(\text{Zr}_{1.75}\text{Nb}_{0.25})\text{O}_{12}$ . The generated 0.63 mol Li vacancies would lead to the stabilization of the cubic phase.
- [22] T. Ohzuku, A. Ueda, J. Electrochem. Soc. 141 (1994) 2972.
- [23] The theoretical electrochemical capacity of  $\text{LiCoO}_2$  is  $137 \text{ mA h g}^{-1}$ , which corresponds to 0.5 Li per  $\text{CoO}_2$ .